Hindawi
Geofluids
Volume 2020, Article ID 4921807, 14 pages
https://doi.org/10.1155/2020/4921807

Research Article

Effect of Particle Size and Solution Leaching on Water Retention Behavior of Ion-Absorbed Rare Earth

Zhong-qun Guo,[1] **Yuan-ming Lai**,[2] **Jie-fang Jin**,[1] **Jian-rong Zhou**,[1] **Zheng Sun**,[1] **and Kui Zhao**[3]

[1]*School of Architectural and Surveying & Mapping Engineering, Jiangxi University of Science and Technology, Ganzhou 341000, China*
[2]*Northwest Institute of Eco-Environment and Resources, Chinese Academy of Sciences, Lanzhou 73000, China*
[3]*Jiangxi Key Laboratory of Mining Engineering, Jiangxi University of Science and Technology, Ganzhou 341000, China*

Correspondence should be addressed to Zhong-qun Guo; guozhongqun_jxust@163.com

Received 15 October 2019; Revised 28 April 2020; Accepted 6 May 2020; Published 26 May 2020

Academic Editor: Baojun Bai

Soil-water characteristic curve reflects water retention behavior of unsaturated soil mass. Particle size and mineral composition can influence water retention behavior of soil mass significantly. To discuss effects of particle size and solution leaching on water retention behavior of ion-absorbed rare earth, soil-water characteristic tests of samples with different particle sizes before and after the solution leaching were carried out by using a pressure plate instrument. Soil-water characteristic curves during drying and wetting were analyzed. A fitting analysis on test data was implemented by the Fredlund&Xing 3 parameter model, the Fredlund&Xing 4 parameter model, and the Van Genuchten model to discuss variation laws of soil-water characteristic parameters in different models. Effects of particle size and solution leaching on water retention behavior of ion-absorbed rare earth as well as action mechanism were investigated. Results demonstrate that given the same matric suction, soil water content decreases gradually with the increase of particle size and content of coarse particles, thus decreasing water retention capacity of soil accordingly. Given the same volumetric water content, matric suction is inversely proportional to particle size. During drying and wetting, the amplitude of variation decreases gradually with the increase of particle size and content of coarse particles. The soil water content after solution leaching is smaller than that before under the same matric suction, indicating that solution leaching can decrease water retention capacity of soil. This is mainly because thickness of the double diffuse layer and pore water pressure are increased as a response to the ion exchange, thus decreasing matric suction.

1. Introduction

Rare earth is adhered onto clay minerals as hydrated cations or carboxyl hydrated cations, which is called ion-absorbed rare earth [1, 2]. Ion-absorbed rare earth mainly distributes in seven provinces and regions in South China. It is the strategic resource that is concerned by the whole world and it is titled as the "mother of new materials" and "industrial gold." Currently, ion-absorbed rare earth is mainly exploited by in situ leaching. In leaching mining, solution of salt leaching agent is injected into the clay ore through the injection well, thus triggering chemical replacement reaction between ammonium ions in the leaching solution and rare earth ions adsorbed on the clay. Rare earth leachate infiltrates in ore body, then converges at the foot of a mountain through the channel for collecting liquid, purified and deposited in hydrometallurgical plant, and finally recovers resources [3, 4]. The in situ leaching is shown in Figure 1. Water retention characteristics of ion-absorbed rare earth can reflect difficulties for pores in soil mass to absorb water and predict penetrating quality of ore body during in situ leaching. They are vital to improve leaching rate of rare earth [5]. During the mineral leaching of ion-absorbed rare earth, hydrated cations adsorbed on clay minerals are changed and there's particle migration in mineral soils. These changes all influence water retention characteristics of soil mass significantly. Studying

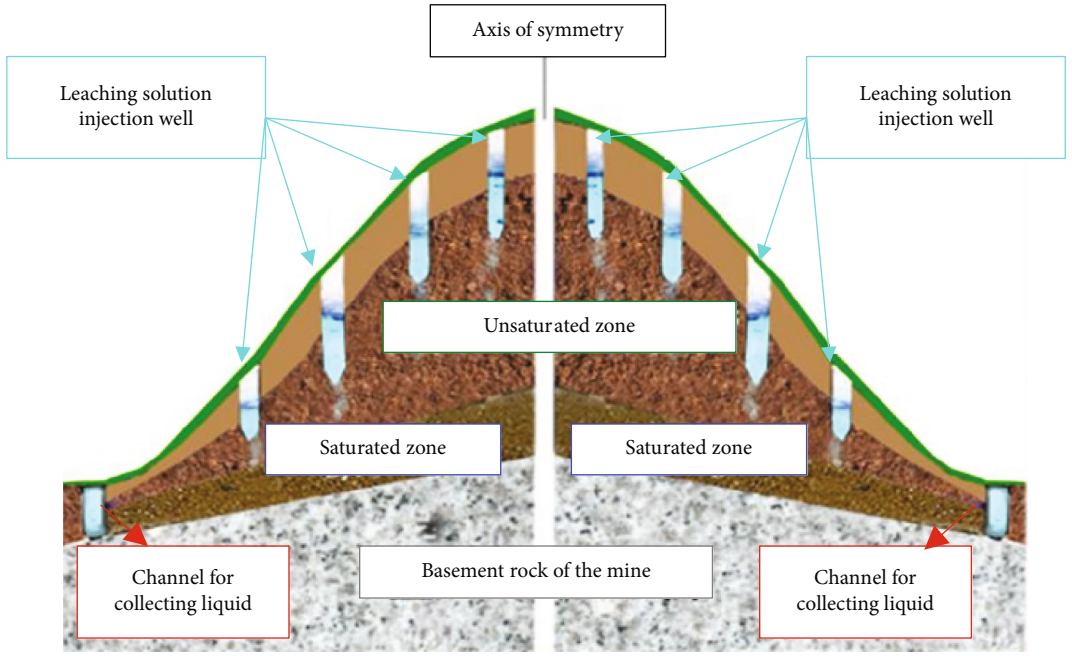

Figure 1: Diagram of in situ leaching.

effects of particle size and solution leaching on ion-absorbed rare earth are conducive to analyze permeability characteristics of ion-absorbed rare earth in different mineral areas and can provide theoretical references for parameter design of liquid injection well network for in situ leaching.

Soil-water characteristic curve (SWCC) is a relation curve between soil water content and suction in soil, and it is an important index to reflect water retention capacity of nonsaturated soil [6]. Soil water content in SWCC can be mass water content or volumetric water content or saturation degree. Suction can be matric suction or total suction. As an explanation to the basic constitutive relation of nonsaturated soil phenomenon, SWCC is sensitive to many factors. Many scholars have carried out abundant studies. Black [7], Tao et al. [8], and Niu et al. [9] discussed influences of mineral components on SWCC. Chiu et al. [10], Rajkai et al. [11], and Chen and Nchimura [12] analyzed influences of particle size on SWCC. Miller et al. [13] and Wang et al. [14] analyzed influences of water content on SWCC. Zhou et al. [15] and Sheng and Zhou [16] discussed effects of dry density on SWCC. Miao et al. [17] and Gong et al. [18] analyzed influences of density and compression on SWCC. Vanapalli et al. [19], Charles and Pang [20], and Wang et al. [21] studied influences of stress history and stress level on SWCC. Salager et al. [22] and Wang et al. [23] considered influences of temperature on SWCC. To sum up, influencing factors of SWCC mainly include internal factors (e.g., mineral composition, particle size and gradation of soil, initial water content, initial dry density, compressivity, and structure) and external factors (e.g., stress history of soil, stress state, temperature, and dry-wet cycle). According to specialty of ion-absorbed rare earth, hydrated cations which are adhered onto clay minerals are changed in in situ leaching process. Currently, there are few studies concerning influences of solution leaching on water retention behavior of ion-absorbed rare earth. In particular, few studies have discussed the variation law of water retention behaviors of rare earth with different particle size after solution leaching. In this study, rare earth samples were collected from the Nanzudong Rare Earth Ore in Jiangxi Province. After screening with particle size and indoor solution leaching, soil-water characteristics of rare earth samples were tested by a pressure plate instrument under different particle sizes and before and after solution leaching. The SWCC curves were fitted by the Fredlund&Xing 3 parameter model, the Fredlund&Xing 4 parameter model, and the Van Genuchten model. Variation laws of soil-water characteristic parameters of different models were verified. Influences of particle size and solution leaching on water retention behavior of ion-absorbed rare earth were discussed, and the relevant influencing mechanism was disclosed.

2. Test Materials and Methods

2.1. Test Materials. Rare earth samples in this experiment were collected in the depth of 0.5~1 m from the Nanzudong Rare Earth Ore in Jiangxi Province (Figure 2). Basic physical indexes of samples are listed in Table 1. The particle size distribution curve of ion-absorbed rare earth is shown in Figure 3. According to classification standards of soils, the rare earth samples are silty clays.

2.2. Experimental Apparatus, Scheme, and Principle. In this experiment, a Geo-Experts stress-related soil-water characteristic curve pressure plate apparatus was applied (Figure 4). It is mainly composed of pressure plate instrument, vertical loading system, pressure control system, and water volume measurement system.

To study effects of particle size and solution leaching on SWCC of ion-absorbed rare earth, rare earth samples were screened by a standard round-hole sieve, thus getting

Figure 2: Sampling site of the Longnan rare earth mine.

Table 1: Basic physical parameters of ion-absorbed rare earth.

Density (ρ) (g·cm^{-3})	Natural water content (θ) (%)	Specific gravity (G_s) (g·cm^{-3})	Void ratio (e)	Liquid limit (w_L) (%)	Plastic limit (w_P) (%)	Plastic index I_p
1.66	16.26	2.68	0.88	40.56	30.27	10.29

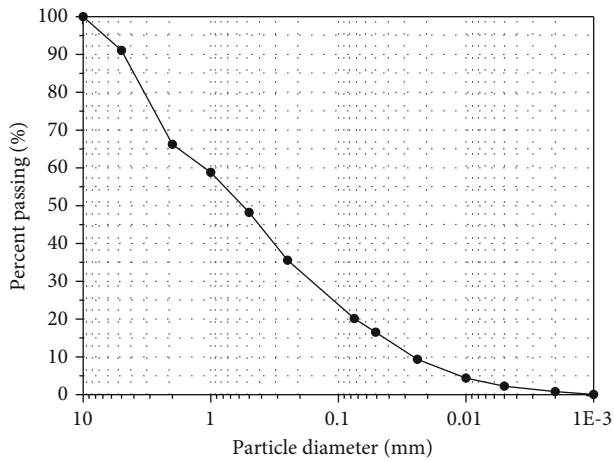

Figure 3: Particle size distribution curve of ion-absorbed rare earth.

samples with different particle sizes and the undisturbed soil size distribution (particles smaller than 0.5 mm account for 48.22% of total soil particles). The sample which contains particles larger than 0.5 mm has poor adhesion like sandy soil and shows significant differences with engineering properties of the collected soils. Therefore, sample with particles larger than 0.5 mm was neglected in the present study. According to the rare earth industrial standard of *Test of Total Ion-phase Rare Earth Based on Chemical Analytic Technique for Ion-absorbed Undisturbed Rare Earth Ore* (XB/T619-2015), the control group of rare earth was put in the ammonium sulfate solution (20 g/L), followed by solution leaching, static deposition, and drying. The experimental design is shown in Table 2. Rare earth samples were remoulded by a ⌀ 70 mm × 19 mm cylinder, with water content and dry density controlled at 15% and 1.3~1.5 g/cm^3. Sieved and dried rare earth was collected to prepare test samples according to preset dry density and water content. Later, the prepared samples were installed into a cutting ring and compacted. The prepared samples were then treated with 24 h of vacuum saturation by a vacuum saturation device (Figure 5) before the experiment. Drying experiment was carried out under 0, 10 kPa, 20 kPa, 50 kPa, 100 kPa, 150 kPa, 200 kPa, 300 kPa, 400 kPa, and 480 kPa. Wetting experiment was conducted after finishing the drying experiment, in which matric suction was decreased level by level to 0. Water would reflow into soil gradually, and data were read after reaching the water equilibrium. Equilibrium standards of samples under single-level matric suction were referred to suggestions of Pham [24]. When the water discharge amount in 24 h is smaller than 0.1 mL, the matric suction is viewed reaching an equilibrium state.

The ceramic plate with high inlet air in the Geo-Experts pressure plate instrument has many uniform micropores. When the ceramic plate is saturated, a shrink film is formed to connect many small pores. The surface tension produced by the shrink film hinders air passing through the ceramic

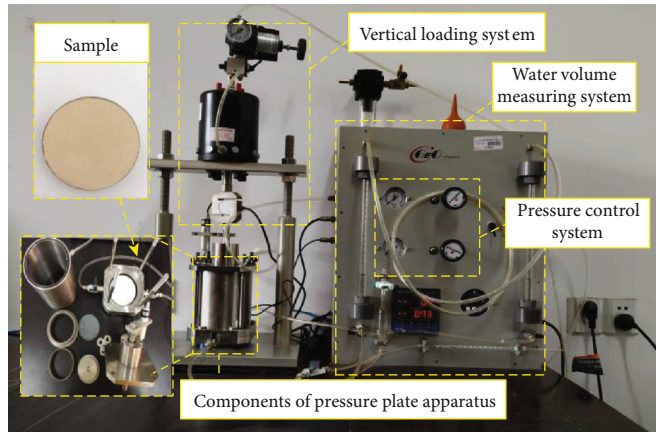

Figure 4: Geo-Experts stress-related soil and water characteristic curve pressure plate apparatus.

Table 2: SWCC test program.

Soil number	Particle size	Leaching conditions	Soil number	Particle size	Leaching conditions
S1	<0.075 mm	Not leaching	L1	<0.075 mm	$(NH_4)_2SO_4$ solution
S2	0.075~0.25 mm	Not leaching	L2	0.075~0.25 mm	$(NH_4)_2SO_4$ solution
S3	0.25~0.5 mm	Not leaching	L3	0.25~0.5 mm	$(NH_4)_2SO_4$ solution
S4	The size of undisturbed soil	Not leaching	L4	The size of undisturbed soil	$(NH_4)_2SO_4$ solution

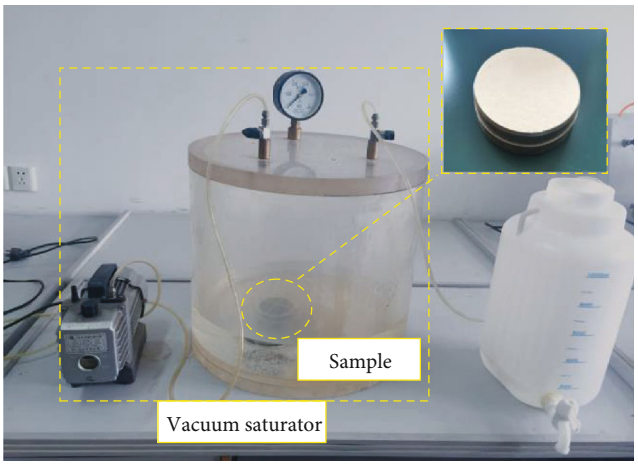

Figure 5: Saturation and preparation of soil sample.

plate. Later, saturated water in ceramic plate drives the convergence between pore water in soil and water in the same measurement system. In this way, the ceramic plate with high inlet air serves as a membrane that prevents air inlet and assures water entrance. The upper surface of ceramic plate bears the air pressure (u_a) and the lower surface bears the pore water pressure (u_w). The pressure difference between the upper and lower surfaces ($u_a - u_w$) is the matric suction of rare earth samples. In the experiment, it is believed that $u_w = 0$ when water in the water volume measurement tube remains constant. Under this circumstance, u_a is equal to the matric suction. At this moment, u_a and variation of water volume in tube (Δv) were recorded.

The initial saturated mass water content of rare earth samples is

$$w_s = \frac{m_t - m_s - m_0}{m_s} \times 100\%, \quad (1)$$

where w_s is the saturated mass water content. m_t is the total mass of cutting ring after vacuum saturation and saturated samples. m_s is the mass of dried samples after the experiment. m_0 is the mass of cutting ring.

In this experiment, mass water content of samples under each level of matric suction was calculated from variations of water volume in the tube at equilibrium of each level of matric suction:

$$w = \frac{m_t - m_s - m_0 - \Delta v_i \rho_w}{m_s} \times 100\%, \quad (2)$$

where w is the mass water content corresponding to a level of matric suction. Δv_i is the variation of water volume in tube at equilibrium of matric suction. ρ_w is the density of water.

The volume water content of samples under different matric suctions is

$$\theta = \frac{w\rho_d}{\rho_w}, \quad (3)$$

where θ is the volume water content and ρ_d is the dry density of soils.

3. SWCC Model and Analysis

3.1. SWCC Model. For studies of SWCC of nonsaturated soils, abundant calculation models were proposed. Common classical models include the Fredlund&Xing 3 parameter model, the Fredlund&Xing 4 parameter model, and the Van Genuchten model.

Expression of the Fredlund&Xing 3 parameter model [25] is

$$\frac{\theta}{\theta_s} = \frac{1}{\{\ln [e + (\psi/a)^n]\}^m}, \quad (4)$$

where θ is the volume water content of soil mass. θ_s is the saturated water content. Ψ is the matric suction of soil mass. a, n, and m are three optimization parameters of the model. The parameter a is related with air inlet. n is a parameter related with drying rate, and it controls slope of the SWCC. m is a parameter related with residual water, and it is correlated with the overall symmetry of curve. This model believes that there is a small θ_r. For the simplification of models, it is hypothesized that $\theta_r = 0$.

The expression of the Fredlund&Xing 4 parameter model [26] is

$$\frac{\theta - \theta_r}{\theta_s - \theta_r} = \frac{1}{\{\ln [e + (\psi/a)^n]\}^m}, \quad (5)$$

where θ_r, a, n, and m are four optimization parameters of the model. Parameters of a, n, and m have the same meaning with those in equation (4). θ_r is the residual water content, and it is not reached in the experiment due to the limited inlet pressure of ceramic plate (the 5 bar ceramic plate in this experiment). Hence, θ_r is gained through data fitting.

The expression of the Van Genuchten model [27] is

$$\frac{\theta - \theta_r}{\theta_s - \theta_r} = \frac{1}{[1 + (a\psi)^n]^m}, \quad (6)$$

where θ is the volume water content of soil mass. θ_s is the saturated water rate. θ_r is the residual water rate. Ψ is the matric suction of soil mass. θ_r, a, n, and m are four optimization parameters of the model. Generally, it is accepted that

$$m = 1 - \frac{1}{n}. \quad (7)$$

The typical nonsaturated SWCC (Figure 6) is composed of three stages, namely, boundary effect zone, transition stage zone, and residual stage zone. The boundary effect zone is a gentile stage of SWCC, in which all soil pores are filled with water and soil particles connect with water. Soil water content is close to the saturated water rate, and properties of soil are similar with those of saturated soil. Air inlet value refers to the matric suction when bubbles began to produce in soil pores. In other words, air begins to enter into the soil mass when the matric suction increases to the air inlet value. This air inlet value refers to the lower boundary of the boundary

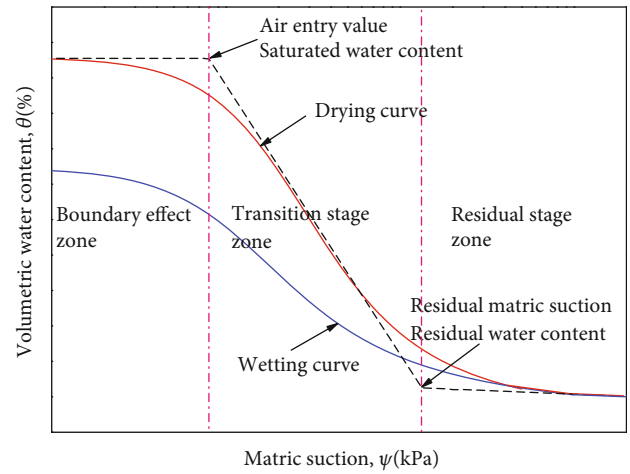

Figure 6: Idealized soil-water characteristic curves.

effect zone. In the transition stage zone of nonsaturated soils, soil water content drops quickly with the increase of matric suction and SWCC is approximately a straight on the semilogarithmic coordinates. The tangential slope of SWCC represents the drying rate, and it reflects water retention capacity of soil mass. In this stage, liquid phase and gas phase are in the double connection and soil mass has complicated properties. In practical engineering, most nonsaturated soils are in the transition stage. The residual water content (θ_r) is the upper boundary of the residual stage. When water content decreases to the residual water content, air in soil pores is connected and pore water only resides in small pores. It has to increase to a significantly high matric suction to support continuous reduction of water content. The residual stage zone is the second gentile stage of SWCC. In this stage, matric suction may influence engineering properties of nonsaturated soils very slightly.

3.2. SWCC and Characteristic Parameter Analysis. SWCCs were fitted by the Fredlund&Xing 3 parameter model, the Fredlund&Xing 4 parameter model, and the Van Genuchten model. The fitting parameters of drying curve are listed in Table 3, and fitting parameters of the water adsorption curve are shown in Table 4. According to fitting results, the coefficient of determination (R^2) of fitting parameters of the drying curve and water adsorption curve ranges between 0.981 and 0.999, indicating that all three models can fit SWCC well. In a word, the Fredlund&Xing 3 parameter model achieves the best fitting accuracy, followed by the Fredlund&Xing 4 parameter model and the Van Genuchten model successively. Although the Fredlund&Xing 3 parameter model has high accuracy, it cannot estimate residual water content directly. In contrast, the Fredlund&Xing 4 parameter model and the Van Genuchten model can estimate residual water content.

Variations laws of drying curves are shown in Table 3. Variation law of the drying curve a: in fitting of the Fredlund&Xing 3 parameter model and the Fredlund&Xing 4 parameter model, values of a decreases with the increase of particle size. Values of a of all samples except for S1 and L1 increase after the solution leaching compared with those

Table 3: SWCC (drying curve) fitting parameters for different particle size conditions.

SWCC model	Parameters	Not leaching				After leaching			
		S1	S2	S3	S4	L1	L2	L3	L4
Fredlund 3	a	42.286	20.136	13.591	21.547	34.234	21.129	16.721	25.654
	n	1.312	1.566	2.249	1.182	1.302	1.482	1.600	1.427
	m	1.612	1.333	0.847	1.367	1.669	1.348	1.242	1.391
	R^2	0.995	0.999	0.993	0.992	0.995	0.999	0.998	0.995
Fredlund 4	a	471.758	33.671	17.119	48.480	478.975	41.222	28.834	49.186
	n	1.0513	1.346	1.909	1.003	1.015	1.249	1.348	1.222
	m	18.566	2.592	1.397	3.055	21.098	3.037	2.549	2.975
	θ_r	9.117	5.221	4.998	3.898	6.941	5.194	4.290	3.229
	R^2	0.997	0.998	0.991	0.990	0.999	0.997	0.996	0.994
Van Genuchten	a	0.001	0.003	0.009	0.010	0.001	0.003	0.005	0.003
	n	2.139	1.979	1.788	1.752	2.127	2.008	1.949	1.914
	m	0.534	0.495	0.441	0.429	0.530	0.502	0.487	0.478
	θ_r	9.146	5.229	4.283	3.992	7.501	5.492	4.039	3.184
	R^2	0.983	0.997	0.991	0.991	0.981	0.995	0.997	0.994

Table 4: SWCC (wetting curve) fitting parameters for different particle size conditions.

SWCC model	Parameters	Not leaching				After leaching			
		S1	S2	S3	S4	L1	L2	L3	L4
Fredlund 3	a	21.286	10.867	12.268	16.385	23.312	19.137	18.407	17.114
	n	1.602	1.500	1.051	0.928	1.305	0.691	0.836	1.202
	m	0.989	1.022	1.539	1.283	1.370	2.069	1.670	1.133
	R^2	0.996	0.992	0.986	0.999	0.998	0.998	0.999	0.999
Fredlund 4	a	44.594	20.094	99.611	41.403	116.467	320.397	90.938	34.176
	n	1.298	1.145	0.628	0.810	1.016	0.562	0.699	1.027
	m	2.732	2.188	4.533	2.831	6.601	9.437	4.993	2.396
	θ_r	8.413	4.722	3.738	3.295	6.461	3.931	3.268	2.768
	R^2	0.993	0.990	0.994	0.999	0.999	0.997	0.999	0.999
Van Genuchten	a	0.003	0.018	0.044	0.024	0.003	0.016	0.026	0.015
	n	1.913	1.740	1.520	1.607	1.982	1.621	1.661	1.625
	m	0.477	0.425	0.342	0.378	0.496	0.383	0.398	0.385
	θ_r	7.851	4.649	3.873	3.795	6.529	4.352	3.713	2.363
	R^2	0.995	0.993	0.991	0.993	0.990	0.990	0.990	0.999

before. Parameter a presents the opposite variation law in the Van Genuchten model. Value of a increases with the increase of particle size. Values of a before and after solution leaching are similar.

The variation law of drying curve n: the value of n in the Fredlund&Xing 3 parameter model and the Fredlund&Xing 4 parameter model increases gradually with the increase of particle size. The value of n after solution leaching is lower than that before. The variation of n is the opposite in the Van Genuchten model. With the increase of particle size, value of n decreases gradually. Values of n in all samples except for S1 and L1 are higher after the solution leaching compared with those before.

The variation law of drying curve m: parameter m presents relatively consistent variation law in the Fredlund&Xing 3 parameter model, the Fredlund&Xing 4 parameter model, and the Van Genuchten model. It is negatively related with particle size. The value of m after solution leaching is higher than that before.

The variation law of drying curve θ_r: this parameter is not involved in the Fredlund&Xing 3 parameter model, but it is found in the Fredlund&Xing 4 parameter model. The

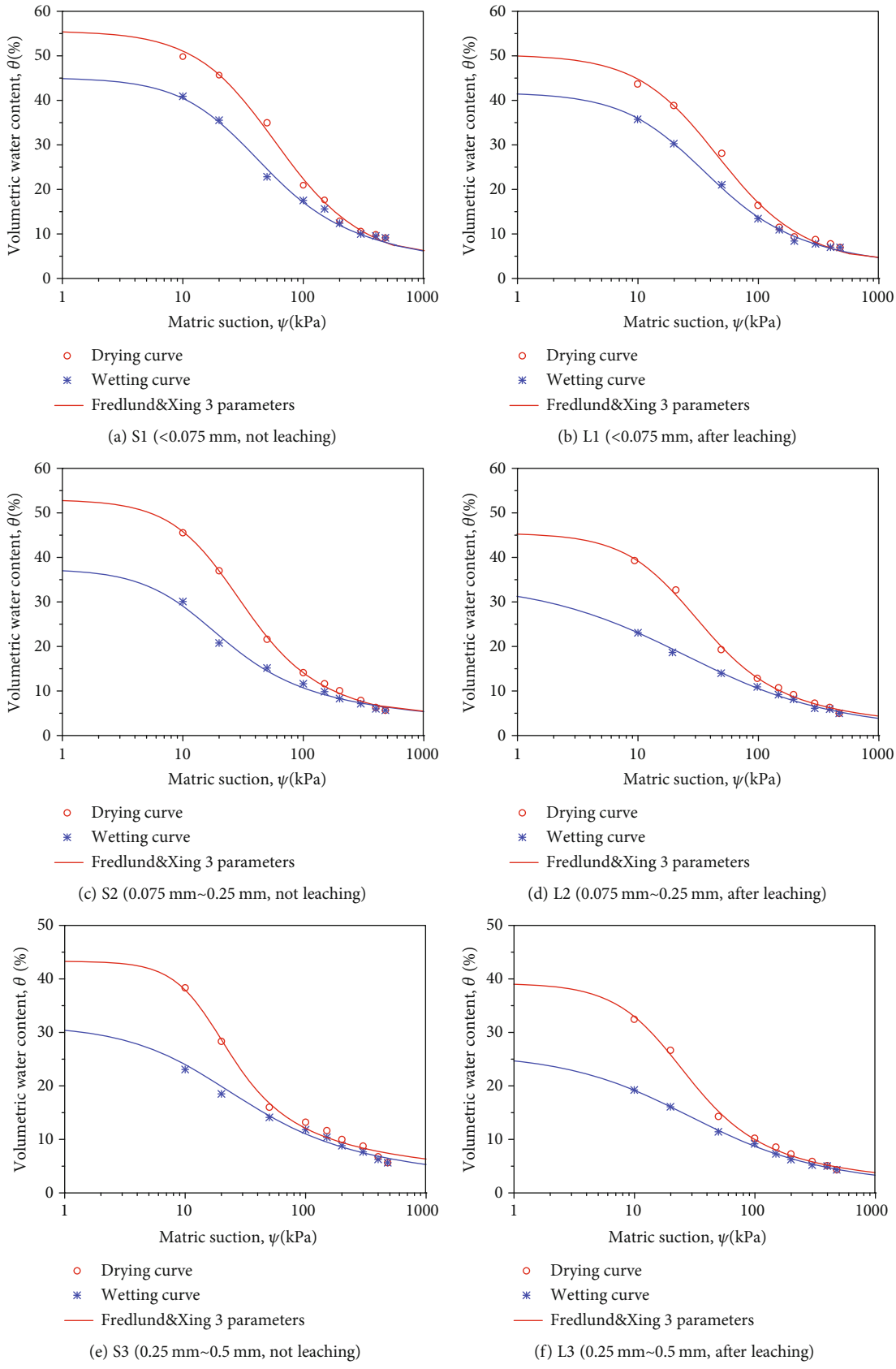

Figure 7: Continued.

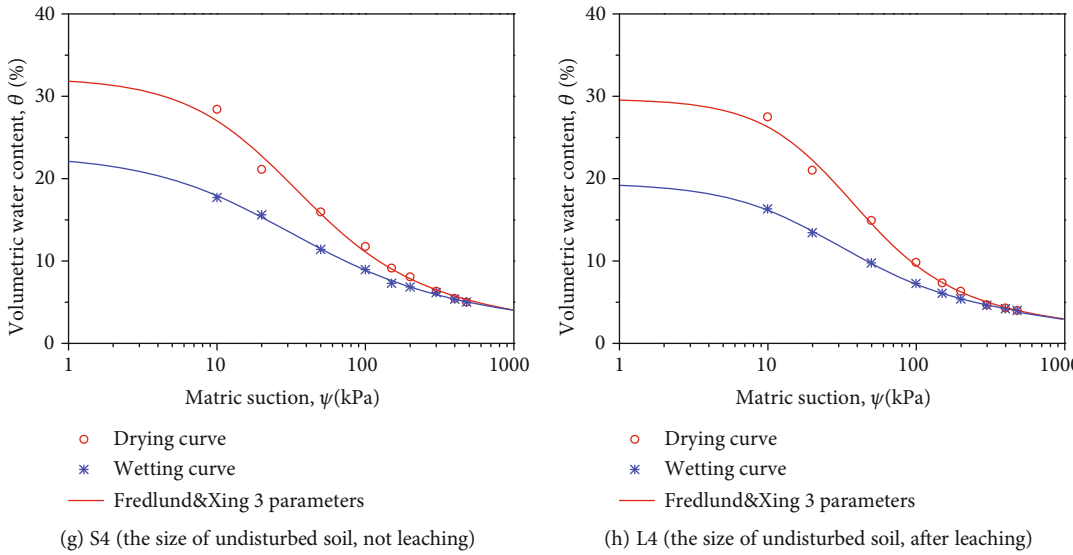

(g) S4 (the size of undisturbed soil, not leaching) (h) L4 (the size of undisturbed soil, after leaching)

Figure 7: Fredlund&Xing soil-water characteristic curves of different soil samples.

parameter θ_r presents relatively the same variation law in the Fredlund&Xing 3 parameter model and the Van Genuchten model. It is negatively correlated with particle size. Moreover, the value of θ_r after the solution leaching is smaller than that before.

It can be seen from Table 4 that variation laws of a and θ_r in the water adsorption curves are similar with those on the drying curve, which are not elaborate again in the present study. The parameter n in the wetting curve is negatively related with particle size, but the parameter m changes slightly, which are different from those of the drying curve.

In 3-parameter and 4-parameter model, the Fredlund&Xing 3 parameter model with the highest fitting accuracy and fewer parameters was applied for graphic analysis of SWCC (Figure 7). Clearly, volume water content of different samples decreases gradually with the increase of matric suction in the drying process. In the wetting process, volume water content of soil samples increases gradually with the decrease of matric suction. Soil samples implemented wetting after drying, but they cannot recover to the original water content completely. Instead, there's certain hysteresis effect which generally can be explained by "capillary tube model" and "contact angle hysteresis effect." In other words, given the same suction, occurrence of water in soil mass in the drying process of evaporation or discharge is higher than that in the wetting process of infiltration and capillary rise. According to analysis, structure, pore diameter distribution, and contact angle of soil samples all change in the drying process, which leads to the failure of recovery of soil samples to the original water content in the wetting process.

4. Analysis on Influencing Factors of Water Retention Behavior

4.1. Effects of Particle Size on Water Retention Behavior. Rare earth samples with three particle sizes (<0.075 mm, 0.075 mm~0.25 mm, and 0.25 mm~0.5 mm) and undisturbed soil grading (particles smaller than 0.5 mm account for 48.22%) were chosen in this study. Drying and wetting curves of rare earth samples with different particle sizes before and after the solution leaching are shown in Figures 8 and 9. Clearly, SWCC moves upward when the particle size is smaller. Given the same matric suction, water content of rare earth samples with smaller particle size and higher content of fine particles is higher and thereby owns the higher water retention capacity. Variation laws of moisture content of these samples are consistent in the drying and wetting processes. With the increase of particle size and decrease of content of fine particles, water content declines gradually and the water retention capacity decreases accordingly. It is found from analysis that with the increase of particle size, the pore diameter is increased accordingly, but air inlet and residual water content decline, thus resulting in the reduction of water retention capacity. It is easy to discover that water content decreases gradually when the matric suction increases from 0 to 200 kPa and the moisture content decreases slowly when the matric suction increases from 200 kPa to 480 kPa. The change amplitude of water content tends to be gentle. When the volume water content is fixed, there is a significant difference in matric suction among samples with different particle sizes. This difference is manifested by the inversely proportional relationship between matric suction and particle size.

Variation of water content of different samples when matric suction increases from 0 kPa to 480 kPa is shown in Figure 10. It can be seen from Figure 10 that the content of coarse particles in ion-absorbed rare earth increases with the increase of particle size and the variation of water content decreases gradually. Before the solution leaching, the variation amplitudes of water content on the drying curve and wetting curve of samples with particle size < 0.075 mm reach as high as 46% and 36%, while variation amplitudes of water content of samples with particle size ranging between 0.25 mm and 0.5 mm are 37% and 24%, respectively. Water content of undisturbed sample on the drying curve and wetting curve is changed slightly (only 27% and 18%), which is related with the increased content of coarse particles and

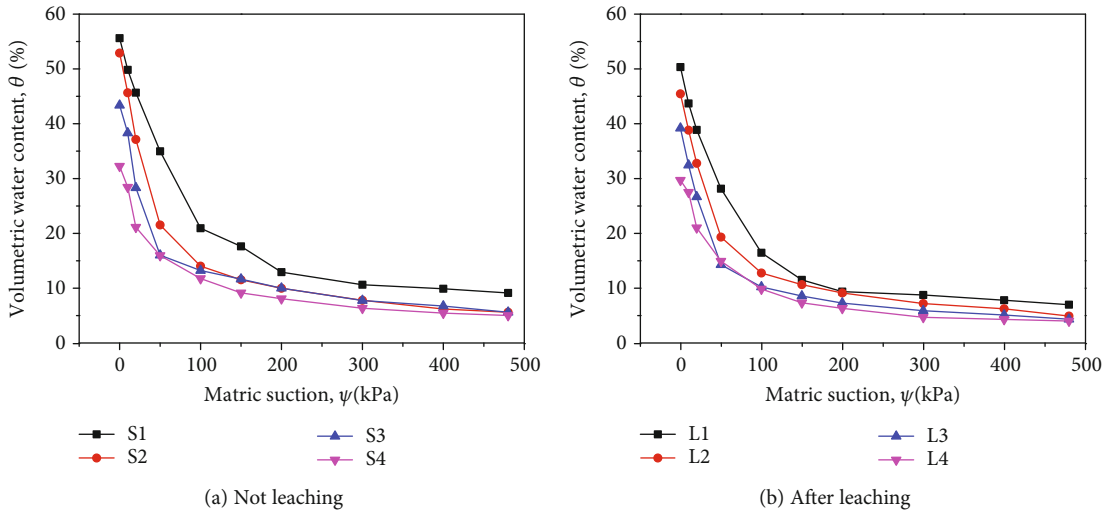

Figure 8: Drying curves of different particle size soil samples.

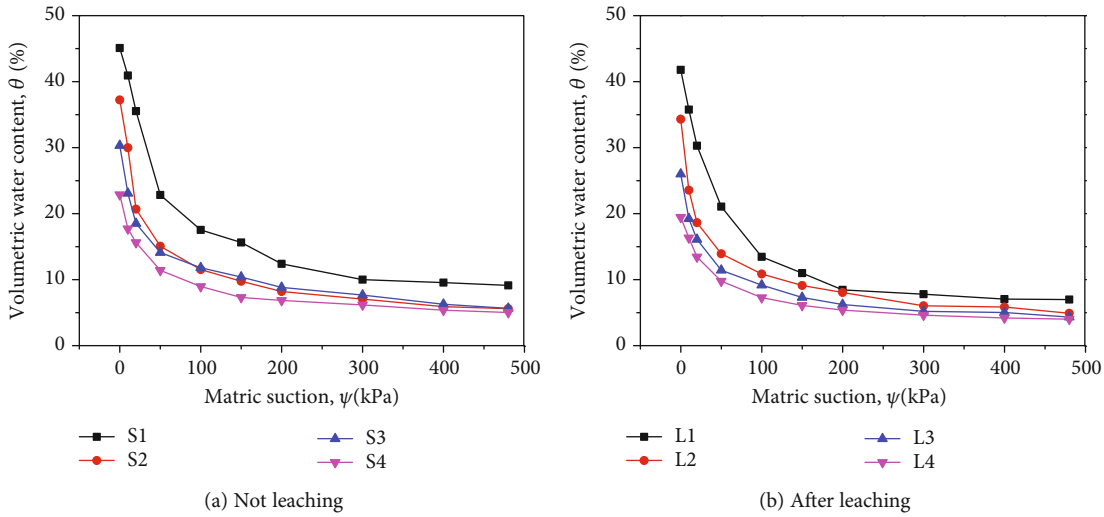

Figure 9: Wetting curves of different particle size soil samples.

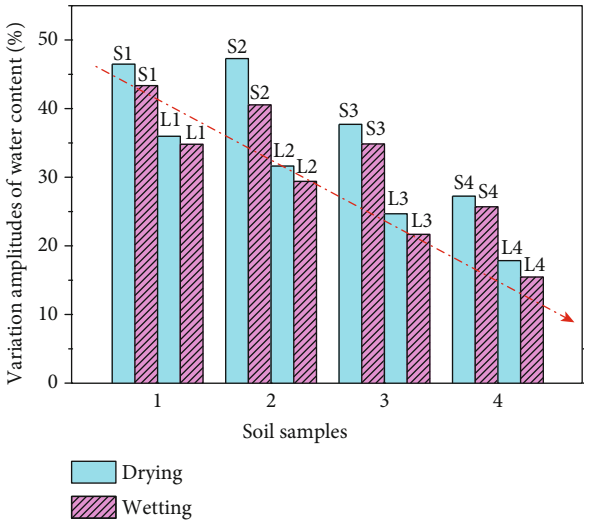

Figure 10: Variation range of water content of different soil samples.

extended range of particle size. After the solution leaching, variation amplitudes of water content on drying curve and wetting curve are 43% and 35% for sample with particle size < 0.075 mm, as well as 35% and 22% for sample with particle size ranging between 0.25 mm and 0.5 mm. The variation amplitudes of water content on drying curve and wetting curve of undisturbed sample are only 26% and 15% after the solution leaching, which are consistent with those before the solution leaching. To sum up, variation amplitude of water content decreases gradually with the increase of particle size and content of coarse particles.

4.2. Influencing Mechanism of Particle Size on Water Retention Behavior. According to the engineering background of in situ leaching, the water content of ore body is low in the early stage of leaching. For unsaturated soil with low water content and high suction value, suction is mainly affected by relatively short-range adsorption which is strongly controlled by the surface properties of soil particles.

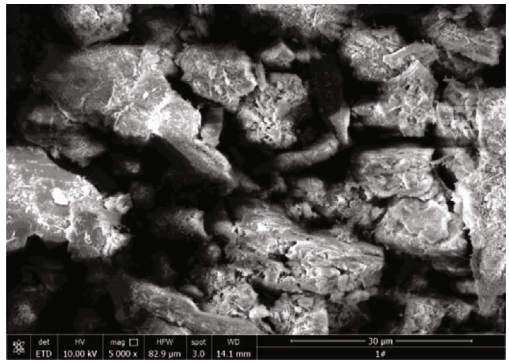

(a) <0.075 mm samples (30 μm, 5000 times)

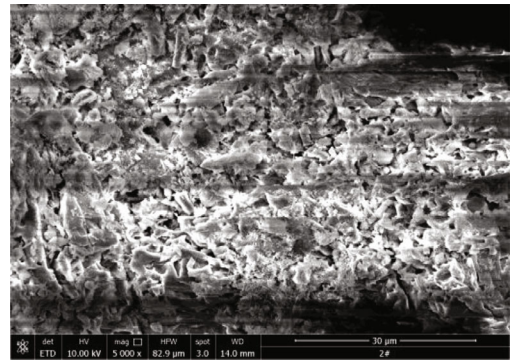

(b) 0.075 mm~0.25 mm samples (30 μm, 5000 times)

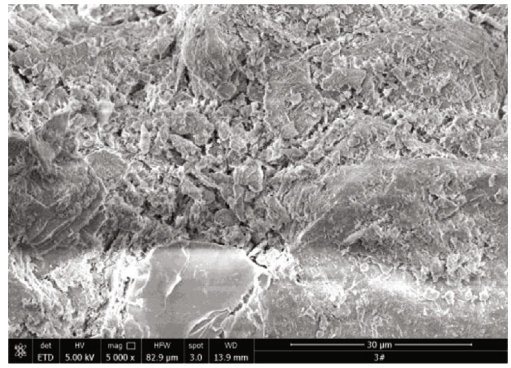

(c) 0.25 mm~0.5 mm samples (30 μm, 5000 times)

Figure 11: Typical SEM images of particle size.

With the continuous leaching process, the water content in the soil increases gradually, and the soil is close to a state of near saturation. And when the unsaturated soil is in high water content, pore water mainly exists in the form of capillary water, and capillary effect is the main reason affecting the water retention behavior. Capillary action is mainly affected by particle size and pore size of soil. Therefore, in the whole process of moisture absorption and drying, the water retention behavior of the soil is mainly affected by the microstructure of soil particles, such as morphology, particle size, pore characteristics, and interparticle relationship.

In order to study the effect of the surface properties of soil particles with different sizes on the water retention behavior of ionic rare earth, three kinds of soil particles with particle size < 0.075 mm, 0.075 mm-0.25 mm, and 0.25 mm-0.5 mm were scanned and photographed with a scanning electron microscope. Because the particle size of mineral soil is small, the particle morphology in the observation surface is not comprehensive if the magnification is too small. Therefore, PCAS system [28] was selected to process and analyze the typical SEM pictures with a magnification of 5000 times, as shown in Figure 11, and the quantitative parameters of microstructure information were shown in Table 5.

It can be seen that soil particles and pore units are mostly dense structures formed by face to face and edge to face, with uneven pore size distribution and high structural dispersion of particles and pores. The surface of soil particles with particle size less than 0.075 mm has large concave opening pores, with obvious pore development, larger pore diameter, and larger specific surface area, which can be used as the channel and storage place for water infiltration. The surface of soil particles with particle size of 0.075-0.25 mm and 0.25-0.5 mm is complex, and the surface opening pores of soil particles with particle size of 0.075-0.25 mm are small and many, which can absorb and hold certain water. The soil particles with particle size of 0.25-0.5 mm are composed of massive agglomerated structure, which are closely arranged. The pore diameter of the surface pore is small, and the pore crossing is shallow. The analysis shows that the smaller the particle size, the larger the opening pore in the particle and the wider the space for free water flow and storage. Therefore, it can be inferred that the smaller the particle size, the more water can be adsorbed by the ionic rare earth particles when the soil is mainly affected by short-range interparticle reaction.

Table 5: Parameters of SEM microstructure (30 μm, 5000 times).

Particle size	Porosity of particle surface	Probability entropy	Mean shape coefficients
<0.075 mm	37.57%	0.9909	0.4248
0.075~0.25 mm	22.97%	0.9887	0.4518
0.25~0.5 mm	10.15%	0.9942	0.4092

From Table 5, it can be seen that the surface porosity of soil particles is 37.57%, 22.97%, and 10.15% when the particle size is less than 0.075 mm, 0.075-0.25 mm, and 0.25-0.5 mm, respectively. With the increase of particle size, the opening porosity of soil particles gradually decreases, which is also consistent with the morphology and porosity of soil particles in the SEM picture. The particle and pore structure of soil is

uncertain and random, and the probability entropy is an index reflecting the orderliness of soil microstructure unit. Its value is between 0 and 1. The larger the probability entropy is, the more chaotic the arrangement of particle and pore unit is, the lower the orderliness of structure is. The change range of probability entropy of soil particles with particle size less than 0.075 mm, 0.075-0.25 mm, and 0.25-0.5 mm is very small, which is between 0.9887 and 0.9942, indicating that the pore distribution of soil samples is chaotic and the orderliness is low at these particle sizes. The mean shape coefficient is an index parameter to describe the shape of soil particles and pore units. The mean shape coefficient represents the geometric shape of particles and pores in the soil microstructure of the whole region. The smaller the mean shape coefficient is, the more complex and narrow the shape of particles and pores is, and the larger the average shape coefficient is, the more circular the shape is. The mean shape coefficients of soil particles in different particle size ranges are not much different, ranging from 0.4092 to 0.4518, indicating that the pore shapes of ionic rare earths are mostly narrow and slender, and the shapes are very complicated. It can be seen that the porosity of particle surface is an effective parameter to analyze the short-range interparticle reactions.

When the water content of soil increases gradually, pore water mainly exists in the form of capillary water, and capillary effect plays a leading role. The saturated volume water content is negatively correlated with particle size. This is because rare earth sample with large particle size has a small porosity. With the increase of matric suction, the variation amplitude of volume water content of rare earth samples with large particle size decreases gradually. This is because pore diameter ratio is relatively small when the particle size is large. This makes the contact of particles more and more tight. According to the Young-Laplace equation

$$u_a - u_w = T_s\left(\frac{1}{R_1} + \frac{1}{R_2}\right), \tag{8}$$

where u_a is the gas-phase pressure, u_w is water-phase pressure, $u_a - u_w$ is the matric suction, T_s is the surface tension of water phase, and R_1 and R_2 are two principal radii of curvature on the interface.

By introducing in the average radius of bending liquid curvature (R_a), equation (8) can be simplified as

$$u_a - u_w = \frac{2T_s}{R_a}. \tag{9}$$

R_a is positively related with particle size and pore size, while the matric suction is negatively correlated with these two parameters. Small particle size is conducive to increase water retention capacity of soil mass. This phenomenon is closely related with double pore structure of ion-absorbed rare earth. Ion-absorbed rare earth in South of Jiangxi Province is mainly adsorbed onto red clay. Clay particles in the clay minerals generally cluster into a silty-level aggregate rather than exist alone. Such aggregation, or called as "particle cluster," is the basic skeleton of clay. Piling pores among different particle clusters are major pores in red clay. Volume of piling pores accounts for about 1/2 of total volume, and volume of pores in particle clusters accounts for about 1/4 of total volume. The rest pores are connected pores. Generation of pore deformation is closely related with deformation of particles and structural connection. Pore distribution of ion-absorbed rare earth has evident double peaks.

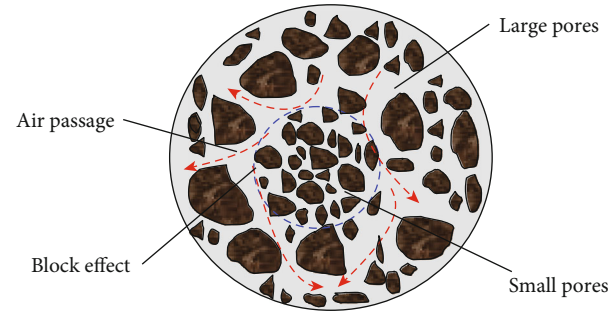

Figure 12: Microscopic structure of ion-absorbed rare earth clay.

In the drying process of ion-absorbed rare earth, big pores are dried firstly due to the small suction. As the drying process continues, some dried pores are connected into a discharge channel. In the next drying process, water flows out firstly from big pores, which forms a microscopic air channel network composed of big pores (Figure 12). Pressure on channels formed by big pores is applied by water in small pores from different directions, thus forming a relatively stable local equilibrium system. This local equilibrium system hinders discharge in small pores. This is known as the "blocking effect." As a result, rare earth sample with larger particle size is easier to form a channel through big pores and the "blocking effect" is developed earlier. The variation curve of water content becomes stable earlier accordingly.

4.3. Effects of Solution Leaching on Water Retention Behavior of Soil Mass. SWCC of different rare earth samples before and after the solution leaching are shown in Figure 13. Both drying curve and wetting curve before the solution leaching are above those after solution leaching. The saturated water content is between 32%~55% before solution leaching and 30%~50% after solution leaching. The minimum water content is 5%~9% before solution leaching and 4%~7% after solution leaching. Rare earth sample before solution leaching has higher water retention capacity than that after solution leaching. Under the same matric suction, volume water content of rare earth sample after solution leaching is lower than that before solution leaching, indicating that solution leaching decreases water retention capacity of soils. Variations of volume water content before and after solution leaching are shown in Figure 10. Variation amplitudes of water content of samples with particle size < 0.075 mm are 46% and 36% before solution leaching, which are decreased to 43% and 35% after solution leaching. Variation amplitudes of water content of samples with particle size ranging 0.075~0.25 mm are 47% and 32% before solution leaching, which are decreased to 41% and 29% solution leaching. Variation amplitudes of water content of samples with particle size ranging 0.25 mm~0.5 mm are 38% and 25% before solution leaching, which are decreased to 35% and 22% after solution leaching.

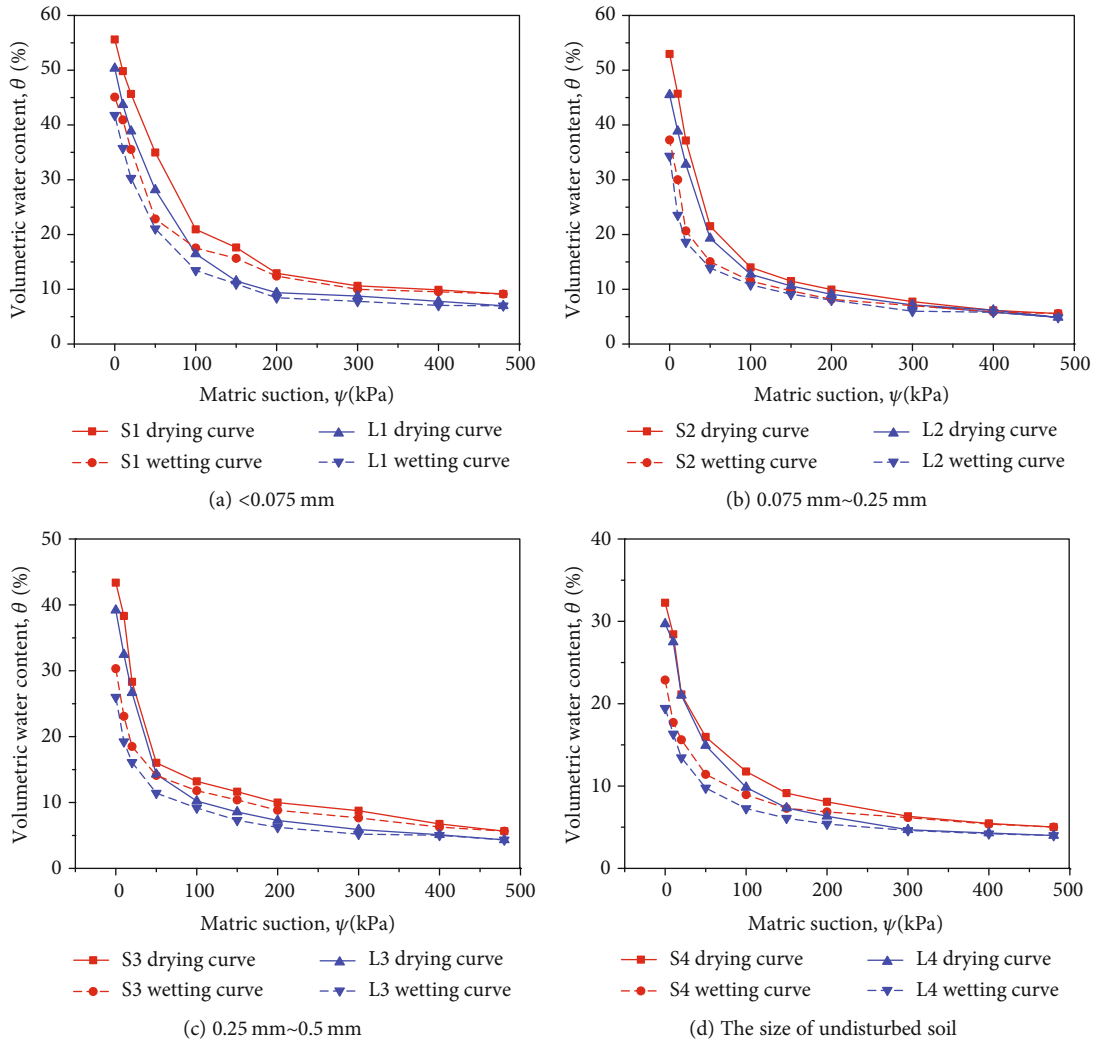

Figure 13: Soil-water characteristic curves of samples before and after the leaching.

Variation amplitudes of water content of undisturbed sample are 27% and 18% before solution leaching, which are changed to 26% and 15% after solution leaching. In a word, moisture content of rare earth samples after solution leaching changes more slightly than that before solution leaching.

4.4. Influencing Mechanism of Solution Leaching on Water Retention Behavior. Silty clay is characteristic of small particle size, large amount of small pores, and high water content. The compression behavior and mechanical properties of silty clay are significantly sensitive to water content. Rare earth ions in ion-absorbed rare earth are adhered onto clay as hydrated cations or carboxyl hydrated cations. According to available data and experimental results, rare earth ions are mainly adhered onto surface of fine soil particles. Interaction between rare earth ions and clay minerals does not change the physical and mechanical properties of clay by changing or destroying the lattice structure of minerals. Instead, they exist in clay minerals as adhesion state and change the bonding state and bonding strength of particles by changing thickness of the double diffuse layer, thus influencing physical and mechanical properties of soil mass.

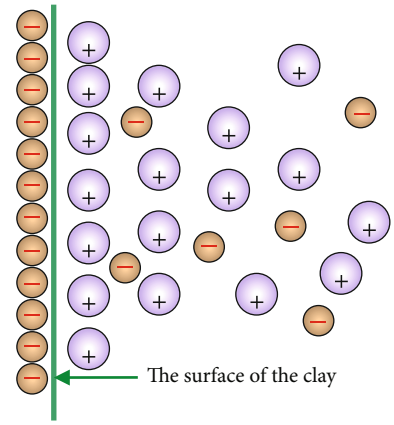

Figure 14: Schematic diagram of double diffuse layers.

Clay particles can only suspend in water rather than dissolve in water. Clay ions have different electric properties in aqueous solution. In the structure of clay, Si^{4+} in the SiO_2 tetrahedral layer might be replaced by Al^{3+} and Al^{3+} in the Alumina octahedral layer might be replaced by divalent ions like

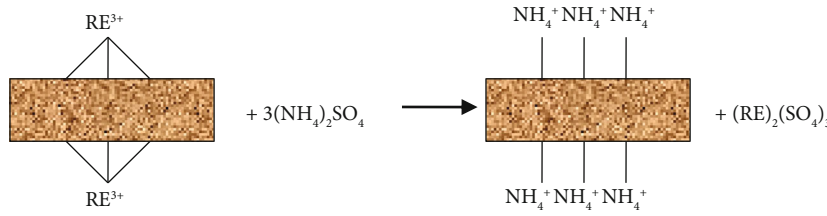

Figure 15: Schematic diagram of ion exchange reaction of mineral leaching.

Mg^{2+} and Fe^{2+}. Due to such replacement, clay particle surface is negatively charged. Some cations, including K^+, Na^+, Ca^{2+}, and RE^{3+}, are adhered onto clay surface as a response to electrostatic attraction. These cations are actually hydrated cations. Hence, a negatively charged cation layer (counterion layer) corresponding to the positively charged hydrated cations is formed on clay particle surface. These two layers are called as the double electric layers (Figure 14). Thickness of the double electric layers is related with valence number of ions in pore water, ion concentration, temperature, and pH.

During solution leaching of ion rare earth, type of ions and ion concentration in the counterion layer are changed. Some ions enter from free solution into the counterion layer, while some ions migrate from the counterion layer to free solution. Such chemical displacement is actually ion exchange. In rare earth exploitation based on in situ leaching, ammonium ions in ammonium sulfate liquid enter into clay minerals and replace rare earth ions RE^{3+} (counterion layer) which are adhered on clay particle surface. This process is shown in Figure 15.

According to the above analysis, thickness of the double diffuse layers is negatively related with valence number of cations in pore water and ion concentration. High-valence rare earth ions are replaced by low-valence ammonium ions during solution leaching. Therefore, rare earth and metal ions like Al^{3+} are displaced through chemical reactions, and ion concentration drops significantly, resulting in the thickening of double diffuse layers. According to water film theory [29], with the increase of thickness of double diffuse layers, the pore water pressure (u_w) increases, while matric suction ($u_a - u_w$) decreases and water retention capacity of ion-absorbed rare earth declines after solution leaching. These are consistent with macroscopic water retention behavior in this experiment. In view of adsorbed water mechanism, hydrate wedge force from the crystal layer to particles increases continuously with the increase of thickness of the water film, resulting in volume expansion. The water film occupies the volume from pores, which decreases water retention capacity accordingly. Moreover, double diffuse layers between particles can intensify deformation of soil mass and the resistance of soil particle skeleton to deformation is enhanced. Macroscopically, this is manifested by difficult compression of the soil particle skeleton. According to the capillary model, pore water in soils is more difficult to be adhered onto soil particle surface. The water content of soil mass declines after solution leaching under the same matric suction, indicating that water retention capacity of soil mass declines after solution leaching.

5. Conclusions

(1) SWCC of ion-absorbed rare earth can be fitted well by the Fredlund&Xing 3 parameter model, the Fredlund&Xing 4 parameter model, and the Van Genuchten model. With respect to fitting accuracy, the Fredlund&Xing 3 parameter model is the best, followed by the Fredlund&Xing 4 parameter model and the Van Genuchten model successively. However, the Fredlund&Xing 3 parameter model cannot estimate residual water content directly, while the Fredlund&Xing 4 parameter model can estimate residual moisture content directly

(2) Given the same matric suction, rare earth samples with smaller particle size or higher content of fine particles have the higher water content and the higher water retention capacity. Given the same volume water content, matric suction is inversely proportional to particle size. Since pore size increases with the increase of soil particle size, the average radius of bending liquid curvature (R_a) increases accordingly, whereas the matric suction declines. With the increase of particle size and content of coarse particles, water content becomes more and more stable in the drying and wetting processes

(3) Given the same matric suction, water content of rare earth samples decreases after solution leaching compared with that before, indicating that solution leaching can decrease water retention capacity of soil. Water content after solution leaching changes less than that before in both drying and wetting processes

(4) According to water film theory, the thickness of the double diffuse layers is increased due to solution leaching, accompanied with increase of pore water pressure and reduction of matric suction. Consequently, the water retention capacity of soil mass after solution leaching decreases. This can reasonably explain the influencing mechanism of solution leaching on water retention behavior of ion-absorbed rare earth

Data Availability

The test data used to support the findings of this study are included within the article. Readers can obtain data supporting the research results from the test data table in the paper.

Conflicts of Interest

The authors declare that they have no conflicts of interest.

Acknowledgments

The study is supported by the National Natural Science Foundation (no. 11902127), the National Undergraduate Innovation Training Program of China (no. 201810407004), and the Project of Science and Technology of Jiangxi Provincial Education Department (no. GJJ180457).

References

[1] X. W. Huang, Z. Q. Long, L. S. Wang, and Z. Y. Feng, "Technology development for rare earth cleaner hydrometallurgy in China," *Rare Metals*, vol. 34, no. 4, pp. 215–222, 2015.

[2] Z. Q. Guo, Y. M. Lai, K. Zhao, J. F. Jie, and G. S. Wang, "Influence range of single hole injection of ionic rare earth for constant head," *The Chinese Journal of Nonferrous Metals*, vol. 28, no. 9, pp. 1918–1927, 2018.

[3] G. S. Wang, Y. M. Lai, P. Long, S. L. Hu, B. G. Hong, and Y. Gui, "Calculation water moisture distribution around injection hole during in-situ leaching process of ion-adsorption rare earth mines," *Chinese Journal of Geotechnical Engineering*, vol. 40, no. 5, pp. 910–917, 2018.

[4] Z. Q. Guo, J. F. Jin, K. Zhao, X. J. Wang, and G. L. Chen, "Status of leaching technology and theory of ion adsorption type rare earth ores," *Chinese Rare Earths*, vol. 39, no. 1, pp. 132–141, 2018.

[5] Q. Zhai and H. Rahardjo, "Estimation of permeability function from the soil–water characteristic curve," *Engineering Geology*, vol. 199, pp. 148–156, 2015.

[6] T. Ma, C. Wei, X. Xia, and P. Chen, "Constitutive model of unsaturated soils considering the effect of intergranular physicochemical forces," *Journal of Engineering Mechanics*, vol. 142, no. 11, article 04016088, 2016.

[7] W. P. M. Black, "A method of estimating the California bearing ratio of cohesive soils from plasticity data," *Geotechnique*, vol. 12, no. 4, pp. 271–282, 1962.

[8] G. L. Tao, J. R. Zhang, X. S. Zhuang, and L. Yang, "A fractal model describing the relation between clay content and soil-water characteristic curve," *Journal of Hydraulic Engineering*, vol. 45, no. 4, pp. 490–496, 2014.

[9] G. Niu, D. A. Sun, C. F. Wei, and L. T. Shao, "Effects of free iron oxide on water retention behavior of lateritic clay," *Chinese Journal of Geotechnical Engineering*, vol. 40, no. 12, pp. 2318–2324, 2018.

[10] C. F. Chiu, W. M. Yan, and K. V. Yuen, "Estimation of water retention curve of granular soils from particle-size distribution— a Bayesian probabilistic approach," *Canadian Geotechnical Journal*, vol. 49, no. 9, pp. 1024–1035, 2012.

[11] K. Rajkai, S. Kabos, M. T. van Genuchten, and P. E. Jansson, "Estimation of water-retention characteristics from the bulk density and particle-size distribution of Swedish soils," *Soil Science*, vol. 161, no. 12, pp. 832–845, 1996.

[12] Y. L. Chen and T. Nchimura, "Influence of particle size on water retention of soils," *Chinese Journal of Rock Mechanics and Engineering*, vol. 35, no. 7, pp. 1474–1482, 2016.

[13] C. J. Miller, N. Yesiller, K. Yaldo, and S. Merayyan, "Impact of soil type and compaction conditions on soil water characteristic," *Journal of Geotechnical and Geoenvironmental Engineering*, vol. 128, no. 9, pp. 733–742, 2002.

[14] Z. Wang, W. L. Zou, and X. Li, "Measurement and application of suction in unsaturated soils," *Journal of Sichuan University(Engineering Science Edition)*, vol. 36, no. 2, pp. 1–6, 2004.

[15] A. N. Zhou, D. Sheng, and J. P. Carter, "Modelling the effect of initial density on soil-water characteristic curves," *Géotechnique*, vol. 62, no. 8, pp. 669–680, 2012.

[16] D. Sheng and A. N. Zhou, "Coupling hydraulic with mechanical models for unsaturated soils," *Canadian Geotechnical Journal*, vol. 48, no. 5, pp. 826–840, 2011.

[17] L. Miao, F. Jing, and S. L. Houston, "Soil-water characteristic curve of remolded expansive soils," in *Unsaturated Soils 2006*, pp. 997–1004, Carefree, Arizona, USA, March 2006.

[18] B. W. Gong, W. W. Ng Charles, and B. Wang, "Influence of stress states on soil-water characteristics of expansive soils," *Rock and Soil Mechanics*, vol. 25, no. 12, pp. 1915–1918, 2004.

[19] S. K. Vanapalli, D. G. Fredlund, and D. E. Pufahl, "The influence of soil structure and stress history on the soil-water characteristics of a compacted till," *Geotechnique*, vol. 49, no. 2, pp. 143–159, 1999.

[20] C. W. W. Ng and Y. W. Pang, "Experimental investigations of the soil-water characteristics of a volcanic soil," *Canadian Geotechnical Journal*, vol. 37, no. 6, pp. 1252–1264, 2000.

[21] D. L. Wang, M. T. Luan, and Q. Yang, "Experimental study of soil-water characteristic curve of remolded unsaturated clay," *Rock and Soil Mechanics*, vol. 30, no. 3, pp. 751–756, 2009.

[22] S. Salager, M. S. el Youssoufi, and C. Saix, "Effect of temperature on water retention phenomena in deformable soils: theoretical and experimental aspects," *European Journal of Soil Science*, vol. 61, no. 1, pp. 97–107, 2010.

[23] C. Wang, Y. Lai, and M. Zhang, "Estimating soil freezing characteristic curve based on pore-size distribution," *Applied Thermal Engineering*, vol. 124, pp. 1049–1060, 2017.

[24] H. Q. Pham, "A volume-mass constitutive model for unsaturated soils, Ph.D. Thesis," University of Saskatchewan, Saskatoon, Canada, 2005.

[25] D. G. Fredlund and A. Xing, "Equations for the soil-water characteristic curve," *Canadian Geotechnical Journal*, vol. 31, no. 4, pp. 521–532, 1994.

[26] D. G. Fredlund, A. Xing, M. D. Fredlund, and S. L. Barbour, "The relationship of the unsaturated soil shear strength to the soil-water characteristic curve," *Canadian Geotechnical Journal*, vol. 33, no. 3, pp. 440–448, 1996.

[27] M. T. Van Genuchten, "A closed-form equation for predicting the hydraulic conductivity of unsaturated soils," *Soil Science Society of America Journal*, vol. 44, no. 5, pp. 892–898, 1980.

[28] C. Liu, B. Shi, J. Zhou, and C. Tang, "Quantification and characterization of microporosity by image processing, geometric measurement and statistical methods: application on SEM images of clay materials," *Applied Clay Science*, vol. 54, no. 1, pp. 97–106, 2011.

[29] M. H. Zhao, X. P. Liu, and W. X. Peng, "Application of aqueous film theory to study of unsaturated soil's suction," *Rock and Soil Mechanics*, vol. 28, no. 7, pp. 1323–1327, 2007.